We are IntechOpen,
the world's leading publisher of Open Access books
Built by scientists, for scientists

6,900
Open access books available

186,000
International authors and editors

200M
Downloads

154
Countries delivered to

Our authors are among the
TOP 1%
most cited scientists

12.2%
Contributors from top 500 universities

CLARIVATE ANALYTICS
BOOK CITATION INDEX
INDEXED

WEB OF SCIENCE™

Selection of our books indexed in the Book Citation Index
in Web of Science™ Core Collection (BKCI)

Interested in publishing with us?
Contact book.department@intechopen.com

CSV-PSO and Its Application in Geotechnical Engineering

Bing-Rui Chen and Xia-Ting Feng

State Key Laboratory of Geomechanics and Geotechnical Engineering, Institute of Rock and Soil Mechanics, Chinese Academy of Sciences
China

1. Introduction

Since the particle swarm optimization (PSO), being a stochastic global optimization technique,was proposed by Kennedy and Eberhart in 1995(Kennedy & Eberhart, 1995; Eberhart & Kennedy, 1995), it has attracted interests of many researchers worldwide and has found many applications in various fields such as autocontrol, machinofacture, geotechnical engineering et al. (Mark & Feng, 2002; Dong et al, 2003; Su & Feng, 2005). There are two main reasons: one is the preferable performance of PSO, the other is its simplicity in operation. In order to avoid the premature and divergence phenomena often occurring in optimization process by using the PSO, especially for multi-dimension and multi-extremum complex problems, as well as to improve the convergence velocity and precision of the PSO to a maximum extent, many kinds of schemes were introduced to enhance the PSO. The following are some representative schemes: inertia weight (Shi & Eberhart, 1998), constriction factor (Eberhart & Shi, 2000), crossover operation (Lovbjerg et al, 2001) and self-adaptation (Lü & Hou, 2004). The PSO modified by introducing the inertia weight or crossover operation or self-adaptation technique has an excellent convergence capability with a decreased velocity of convergence. The PSO with a constriction factor can reach the global goal quickly, but the divergence phenomenon sporadically occurs in the optimized solutions.

So we proposed an improved PSO, named CSV-PSO, in which flight velocity limit and flight space of particles are constricted dynamically with flying of particles (Chen & Feng, 2005). A great deal of numerical calculation indicates CSV-PSO has a faster convergence velocity, greater convergence probability and is a more stable. But this algorithm with a random number generator having time as its random seed may obtain different goal values at different running time. It is difficult to determine uniqueness of solution, especially for complicated engineering problem. So a random number generator with mixed congruential method is introduced to solve uncertainty of solution, and its random seed can be set artificially. To indicate advantage of the proposed algorithm, it is compared with other modified vertions and sensitivity analysis is carried out for its several important parameters, which the five benchmark functions are as examples. The results show CSV-PSO with a new random number generator is excellent. Back analysis which is based on monitoring information with numerical method is a very time-consuming job in geotechnical

engineering field. It is necessary to introduce a scheme for improving calculation efficiency. A parallel strategy is adopted, and a parallel CSV-PSO with master-slave mode, called PCSV-PSO, is proposed. Finally, rheological parameters of soft and weak rock mass, as an engineering practical example, are identified using back analysis of displacement based on PCSV-PSO, at the No. 72 experimental tunnel, left bank of Longtan hydropower station, China. The results show that the proposed method is feasible, efficient and robust in multi-parameter optimization and is a new analysis tool for engineering application.

2. PSO

In PSO algorithm, the birds are abstractly represented as particles which are mass-less and volume-less and extended to D dimensional space. The position of the particle i in the D dimensional space is represented by a vector $\vec{X_i} = (X_{i1}, X_{i2}, \cdots, X_{iD})$, and the flying velocity is represented by a vector $\vec{V_i} = (V_{i1}, V_{i2}, \cdots, V_{iD})$. The vectors $\vec{P_i} = (P_{i1}, P_{i2}, \cdots, P_{iD})$ and $\vec{P_g} = (P_{g1}, P_{g2}, \cdots, P_{gD})$ are the optimal position of the particle i recognized so far and the optimal position of the entire particle swarms recognized so far, respectively. The position of each particle in the D dimensional space, $\vec{X_i}$, is a tentative solution in the problem space. The fitness of the model, representing applicability of the $\vec{X_i}$, can be obtained by substituting $\vec{X_i}$ to the target function. Therefore, the search procedure of PSO algorithm depends on interaction among particles. The position and velocity of the particle i can be updated as Eq.(1) and (2) (Kennedy & Eberhart,1995; Shi & Eberhart,1998) .

$$V_{id} = wV_{id} + c_1 r_1 (P_{id} - X_{id}) + c_2 r_2 (P_{gd} - X_{id}) \tag{1}$$

$$X_{id} = X_{id} + V_{id} \tag{2}$$

In which, w is inertia weight; c_1 and c_2 are constants for learning, $c_1 > 0$, $c_2 > 0$; r_1 and r_2 are random numbers in [0,1]; $d = 1,2, \cdots, D$.

The basic PSO algorithm has advantages of simple operation and convenient application. However, as other optimization algorithms such as genetic algorithms, the basic PSO algorithm has also the problems of premature and slow convergence, therefore, an improvement in accuracy is needed.

3. CSV-PSO

In order to improve the convergence velocity and precision of the PSO algorithm, the CSV-PSO algorithm which can adjust inertia weight, flight velocity limit and flight space of particles dynamically and nonlinearly was proposed. This Algorithm has been documented in our early paper (Chen & Feng, 2005). Random Number Generator and parallel CSV-PSO algorithm (PCSV-PSO) are described in detail and CSV-PSO algorithm is briefly introduced in this section.

3.1 Random Number Generator

Random number is the crucial factor for the performance of swarm intelligence algorithms, and a good random number generator can always get twice the result with half the effort. A algorithm with random number generator that time is as its random seed always tends to give different results in different runtime, which brings troubles for the final determination of solving proposal of engineering problems. To resolve this problem, a random number generator with the mixed congruential method is proposed in the paper. This generator can generate random numbers of uniform distribution in the interval of (0, 1) and random seed can be set artificially. A great deal numerical results show that this technique is excellent. The process of the generation of random seeds is as following.

The iterative formulae of the mixed congruential method are:

$$x_{i+1} = (\lambda x_i + c)(\mathrm{mod}\, M) \tag{3}$$

$$r_{i+1} = x_{i+1} / M \tag{4}$$

Where λ 、 x_0 、 c and M are constants and can set beforehand, x_{i+1} is the remainder of M divided by $\lambda x_i + c$ and r_{i+1} is a random number within the interval of (0, 1). Each random number generated by the mixed congruential method in accordance with an index number and is stored in an internal array after random number generator is initialized. If random number is needed, the random number generator will firstly call the computing function of the mixed congruential method to generate random integer used as index, then the random number is picked up from internal array in terms of the index, finally the random number generator carries out the mixed congruential method again to update the internal array. The random number sequences obtained by this method are much better than those obtained by common mixed congruential methods. The C language codes which are used to describe the above mentioned method are as follows:

```
double CRandom::ran(long *idum)
{
// idum is random seed
const long M1=259200l;
const long IA1=7141l;
const long IC1=54773l;
const double RM1 = (1.0/M1);
const long M3=243000l;
const long IA3=4561l;
const long IC3=52349l;
static long ix1,ix2,ix3;
static double r[98];
double temp;
static int iff=0;
long j;  //int j;
if (*idum < 0 || iff == 0) {
ff=1;
x1=(IC1-(*idum)) % M1;
ix1=(IA1*ix1+IC1) % M1;
```

```
ix3=ix1 % M3;
for (j=0;j<=97;j++) {
 ix1=(IA1*ix1+IC1) % M1;
 r[j]=ix1*RM1;
}
*idum=1;
}
ix1=(IA1*ix1+IC1) % M1;
ix3=(IA3*ix3+IC3) % M3;
j=(97*ix3)/M3;
if (j > 97 || j < 0) cout<<"RAN: This cannot happen."<<endl;
temp=r[j];
r[j]=ix1*RM1;
return (double)temp;
}
```

3.2 CSV-PSO

3.2.1 Inertia Weight

The notion of inertia weight parameter is introduced by Shi and Eherhart (Shi & Eberhart, 1998) to control the impact of the previous history of velocities on current velocity. This enables to influence the tradeoff between global and local exploration abilities of the particles. A larger inertia weight facilitates global optimization, while smaller inertia weight facilitates local optimization. A decreasing inertia weight with iteration was introduced in terms of a linear formulation by Shi and Eherhart. A equation for ineria weight modification is proposed by a great deal numerical simulations here as following:

$$w = w_0 (1 - (\frac{k-1}{k})^n)$$

(5)

Where w_0 is a constant given; k is number of fly; n is a constant determined for fitness function in global optimum problem.

3.2.2 Limit of the Flying Velocity

The limit of the flying velocity of the particles is an important factor that affects velocity of convergence of the PSO (Eberhart & Shi, 2000). In fact, a good limitation is of advantage to both velocity and precision of convergence. Here we adopt Eq. (6) and (7) to determine limit of the flying velocity of the particles.

In which, $Up_{\max d}$, $Down_{\min d}$, $V_{\max d}$, $V_{\min d}$ are the upper limit and the lower limit of the position and the upper limit and lower limit of the velocity at d dimensional space, respectively, $d = 1,2,\cdots,D$. The parameter α can be determined using Eq. (8).

$$V_{\max d} = \alpha (Up_{\max d} - Down_{\min d})$$

(6)

$$V_{\min d} = \alpha (Down_{\min d} - Up_{\max d})$$

(7)

$$\alpha = \alpha_0 (1 - (\frac{k-1}{k})^m)$$

(8)

Where α_0 is a given constant; k is number of fly; m is a constant determined for fitness function in optimum problem.

3.2.3 Compression of Search Space

Particles approach excellent domain step by step with the "flying" of particles continuously. If domain for searching global goal is compressed properly in the "flying" process, convergence of PSO will be accelerated. So the equations for compressing search space are introduced as following:

$$Up'_{\max d} = \beta_0 (Up'_{\max d} - G_{cd}) + G_{cd} \tag{9}$$

$$Down'_{\min d} = \beta_0 (Down'_{\min d} - G_{cd}) + G_{cd} \tag{10}$$

Where $0 < \beta_0 < 1$; $Up'_{\max d}$, $Down'_{\min d}$ and G_{cd} are the upper limit, the lower limit and the geometrical center of gravity of particle swarm in the d dimensional direction of the compressed space, respectively; G_{cd} can be calculated using Eq. (11) (Clerc, 1999) as

$$G_{cd} = \left. \sum_{i=1}^{N_{pop}} x_{id} \right/ N_{pop} \tag{11}$$

Where N_{pop} is the population of the particles; x_{id} is position of the No. i particle in the d dimensional direction.

3.2.4 CSV-PSO Algorithm

In process of space compressing, on the one hand the global optimum probably is out of searching ranges so that the global goal is unable to be found, on the other hand flying velocity of particles is decreased, which can be obviously by Eq. (6) and (7), and the performance of the algorithm jumping out local solution is reduced. Therefore, searching space and flying velocity limit can't be compressed without limitations. The compression should is finished when limit of flying velocity is less a small given value. Particles may fly to the same local value with "flying" of particles continuouly. Therefore, stagnancy phenominon may occur in PSO (The so called stagnancy phenominon is that best particle doesn't move toward any direction during "flying" of particles). If no measure is taken, the PSO may need a long time to get rid of the particle stagnancy or traps into local goal forever. Initializing partial particles' position and flying velocity is an efficient method again when the present best particle is not move to global goal within some "flying" times. The particles are divided into two parts: one part are given new position and flying velocity in compressed space, the other is initialized in original space. These ensure that the algorithm have a better convergence precision and a faster convergence velocity. The whole optimized process of CSV-PSO is as following:

Step 1: Initialize the inertia weight w_0, learning factors c_1 and c_2, the population of group N_{pop}, number of stagnancy generation N_s, constants α_0 and β_0, and end remark of evolutionary process N_g and ε_0, go to Step 2.

Step 2: The positions of the particles are randomly generated in $\left[\overrightarrow{Down_{\min}}, \overrightarrow{Up_{\max}} \right]$. The limitations of flying velocity of the particles, $\overrightarrow{V_{\min}}$ and $\overrightarrow{V_{\max}}$, are calculated using Eqs. (6) and (7). And then, the flying velocity of the particles is initialized randomly in $\left[\overrightarrow{V_{\min}}, \overrightarrow{V_{\max}} \right]$. Set up $n = 0$, go to Step 3.

Step 3: Substitute X_i to goal function to calculate the fitness of the No. i particle $f(X_i)$. The global optimal position of the particle swarm group $\overrightarrow{X_g^b}$ and the best position of particle individual during the fly $\overrightarrow{X_i^b}$ are determined according to the fitness $f(X_i)$, go to Step 4.

Step 4: Substitute $\overrightarrow{X_g^b}$ to goal function to calculate the best fitness of this flying f_g^b. If f_g^b is obviously better than that of the former flying, go to Step 5. Otherwise, go to Step 6.

Step 5: If $f_g^b < \varepsilon_0$ or $n > N_g$, then the optimization process ends. Otherwise, let $n = n+1$, the position and flying velocity of the particles are updated by using Eqs. (1) and (2) and insured in $\left[\overrightarrow{Down_{\min}}, \overrightarrow{Up_{\max}} \right]$ and $\left[\overrightarrow{V_{\min}}, \overrightarrow{V_{\max}} \right]$, go to Step 3.

Step 6: Use Eq.(5) to dynamically update w. If f_g^b is not changed in all N_s continuously, go to Step 7. Otherwise, go to Step 5 ;

Step 7: Use Eq.(6) and (7) to modify dynamically the limit of flying velocity of the particles, and use Eqs. (9) and (10) to compress the search space of the particles, go to Step 8.

Step 8: The particles are divided into two parts. One part is initialized in the compressed space $\left[\overrightarrow{Down_{\min}'}, \overrightarrow{Up_{\max}'} \right]$ and another part is renewedly initialized in the original space $\left[\overrightarrow{Down_{\min}}, \overrightarrow{Up_{\max}} \right]$, go to Step 5.

3.3 Performance Analysis of CSV-PSO

To test performance of the CSV-PSO with random numbers generated by the mixed congruential method, five nonlinear benchmark functions, whose basic characteristics and properties are listed as table 1, are used. To facilitate the description of the two CSV-PSO algorithms: one uses time as random seed, the other utilizes mixed congruential method to produce random numbers and random seed can be set artificially, the former is called CSV-PSO1 and the latter is named CSV-PSO2.

3.3.1 Convergence Velocity

For comparison, in all cases and all improved PSO algorithms, the population size was set to 30; the maximum number of iteration was set to 10,000; the factors for learning c_1 and c_2 are both set to 2.0 and five benchmark functions are set as shown in table 1. Inertia weights of CSV-PSO1 and CSV-PSO2 are set to 1.0 at the beginning of the run, different from that of Eberhart and Shi (Eberhart & Shi, 2000) and they can be decreased to a very small positive value by Eq. (5) .Newly introduced parameters N_s, α_0 and β_0 are 50,0.9 and 0.8 respectively and the α calculated by Eq. (8) can't be less 0.1. It is special for function *Schaffer's f₆* that

α_0 was set to 0.5 in CSV-PSO1. Each version of PSO is run 20 times for each test function, among them the first four are run randomly and the last are run with random seed from 5 to 950 by an increment 50 for each run. Average number of iteration and ranges of iteration number for five functions are listed in table 2 where each method is convergent by 20 runs. The result of the former three versions is gained by Eberhart and Shi (Eberhart & Shi, 2000), and the fourth was from our reference (Chen & Feng, 2005).

Name	Expression	Dimension	Ranges	Optimum	Goal
Sphere	$f_0(x) = \sum_{i=1}^{n} x_i^2$	30	$[-100,100]^n$	0	0.01
Rosenbrock	$f_1(x) = \sum_{i=1}^{n-1} (100(x_{i+1} - x_i^2)^2 + (x_i - 1)^2)$	30	$[-30,30]^n$	0	100
Rastrigrin	$f_2(x) = \sum_{i=1}^{n} (x_i^2 - 10\cos(2\pi x_i) + 10)$	30	$[-5.12,5.12]^n$	0	100
Griewank	$f_3(x) = \frac{1}{4000} \sum_{i=1}^{n} x_i^2 - \prod_{i=1}^{n} \cos(\frac{x_i}{\sqrt{i}}) + 1$	30	$[-600,600]^n$	0	0.1
Schaffer's f_6	$f_6(x) = 0.5 + \frac{(\sin\sqrt{x_1^2 + x_2^2})^2 - 0.5}{(1 + 0.001(x_1^2 + x_2^2))^2}$	2	$[-100,100]^n$	0	10^{-5}

Table 1. Five benchmark functions for testing

		Inertia Weight	Constriction Factor (V_{max}=100000)	Constriction Factor ($V_{max}=X_{max}$)	CSV-PSO1	CSV-PSO2
Sphere	N_{aver}	1537.8	552.05	529.65	680.15	599.45
	N_r	1485-1615	503-599	495-573	456-935	473-842
Rosen-brock	N_{aver}	3517.35	1424.1	992	203.2	297.05
	N_r	2866-4506	475-4793	402-1394	108-545	130-732
Rastr-igrin	N_{aver}	1320.9	6823	213.45	215.45	707.05
	N_r	743-1704	233-7056	161-336	86-726	100-2060
Griew-ank	N_{aver}	2757.7	437	312.6	510.45	622.26
	N_r	2638-3035	384-663	282-366	385-707	318-3647
Schaf-fer's f_6	N_{aver}	512.35	430.55	532.4	111.9	466.65
	N_r	339-748	105-899	94-2046	3-332	41-1981

Table 2. Convergence velocity of several versions of PSO for the five test functions

N_{aver} and N_r are average value and ranges of convergent iteration number among 20 runs respectively in the table 2. For example, N_{aver} and N_r are average value and ranges of iteration number of 17 runs separately when there are 3 divergent runs in 20 runs. If one run doesn't reach the goal in 10000 iterations, this run is regarded as divergence. Where constriction factor version (V_{max}=100000) and improved constriction factor version ($V_{max}=X_{max}$) have one divergence

of 20 runs for function *Rastrigrin* for respectively; Constriction factor version (V_{max}=100000) has 3 divergences, improved constriction factor version (V_{max}=X_{max}) has one divergence, and CSV-PSO2 has one divergence for function *Griewank* among 20 runs. In comparison with other versions, CSV-PSO has a better convergence velocity, and is more stable. Performance of CSV-PSO2 is a bit worse than that of CSV-PSO1, but it is better than other versions, its random seed can be set artificially and unique solution can be obtained at each run using CSV-PSO2.

3.3.2 Precision of Convergence

A 30-dimension function *Rosenbrock*, whose variables are in interval of [-10, 10], is taken as an example for analyzing convergence precision of several improved versions of PSO. For comparison, in all versions of PSO, the population size was set to 20; the maximum number of iteration was set to 2000; the factors for learning c_1 and c_2 are both set to 2.0; Initial inertia weights of CSV-PSO1 and CSV-PSO2 are 1.0, which are different from that of other versions. Newly introduced parameters N_s, α_0 and β_0 are 50, 0.9 and 0.8 respectively. Each version of PSO is run 20 times for test function, the first five are run randomly and the last is run with random seed from 5 to 950 by an increment 50 for each run. Average value of 20 runs for each version is listed in table 3. The result of the former two columns is gained by Clerc and Kennedy (Clerc and Kennedy, 2002), the third and the fourth are from the literature (Ke et al., 2003), the fifth and the last are obtained by CSV-PSO1 and CSV-PSO2 respectively. In fact, when the goal of 0.4 is obtained using the proposed method in the paper, average iteration number of 20 runs is just 913.24. So the proposed method has a better velocity and precision of convergence for function *Rosenbrock*.

Constriction factor1	Constriction factor2	Inertia weight	MPSO	CSV-PSO1	CSV-PSO2
50.193877	39.118488	40.602026	30.316998	0.048169	0.001070

Table 3. Optimal precision of several versions of PSO for function *Rosenbrock*

3.4 Sensitivity Analysis of Parameters

Sensitivity analysis of parameters, on the one hand, can make algorithm do its better, and on the another hand, can offer reasonable basis for parameter selection. There has been a lot of research about basic parameter analysis of the PSO algorithm, and now we just analyze the sensitivity of several parameters used by the CSV-PSO algorithm. The five benchmark functions are selected as testing examples, whose characteristics and properties are shown in table 1.

3.4.1 Random Seeds

The initial population of PSO algorithm is generated randomly, and the main operations (such as the updating of the position and velocity of particles etc.) of PSO contain random factors. So, random seed must have some effect on algorithm performance. But how does it affect and are there any lows to follow? Effect of Random seed on CSV-PSO is analyzed and discussed based on five benchmark function in table 1 as following.

Parameters setting of CSV-PSO: the population size was set to 20; the maximum number of flight is 2000 times; the factors for learning c_1 and c_2 are both set to 2.0; initial inertia weights is 1.0; number of stagnancy iteration is 10; constant α_0 and β_0 is set to 0.9 and 0.8 respectively the α obtained by Eq. (8) can't be less 0.1; random seed is from 0 to 1000 by an increment 50 for each scheme; goal values of five functions are listed as table 1 and number of maximum iteration is the terminating condition of algorithm.
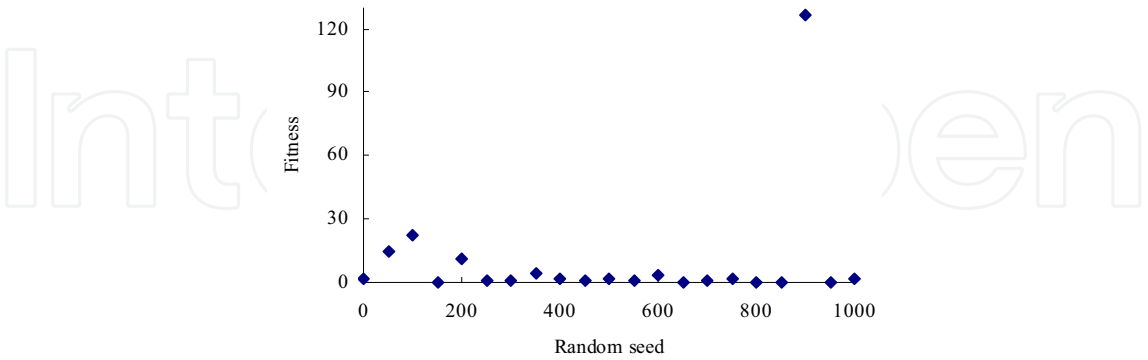
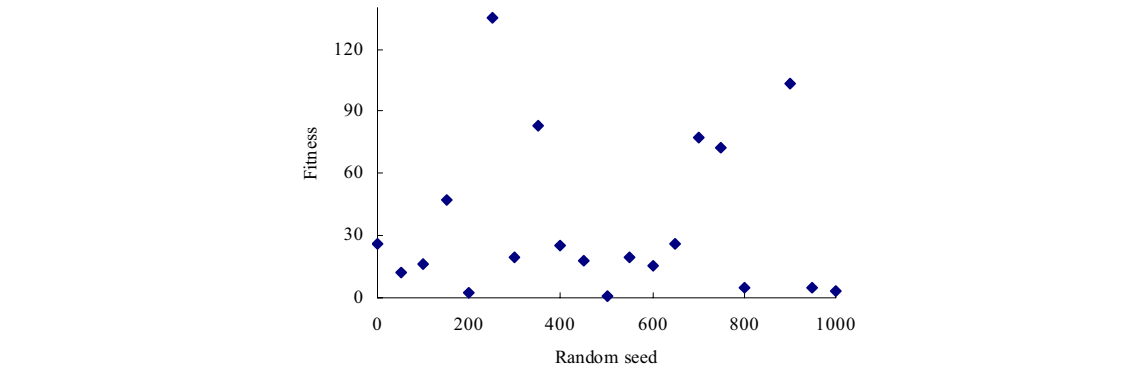Figure 1. Effect of different random seed on precision of function *Sphere*

Figure 2. Effect of different random seed on precision of function *Rosenbrock*
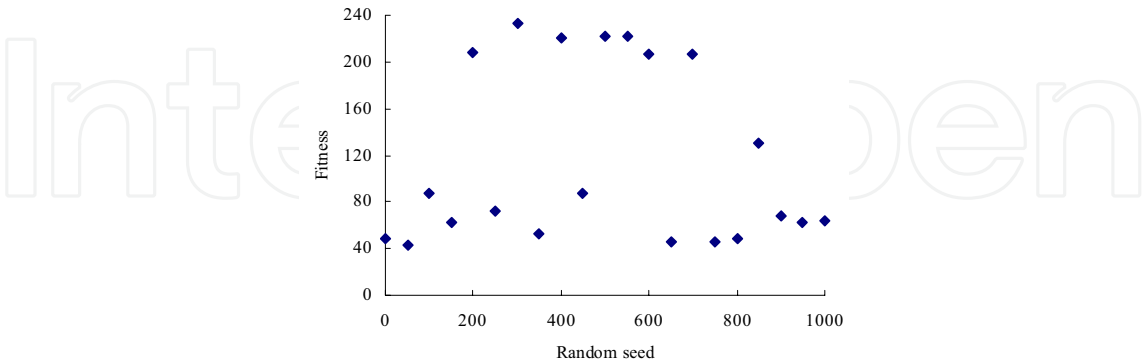

Figure 3. Effect of different random seed on precision of function *Rastrigrin*
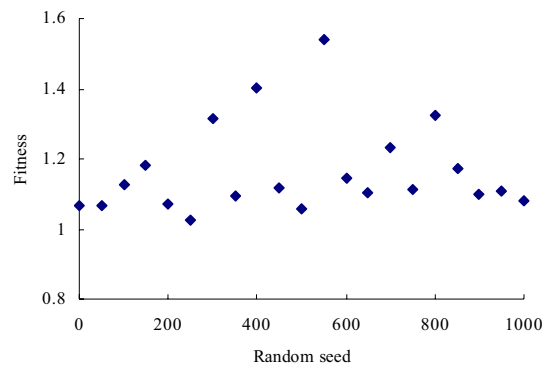
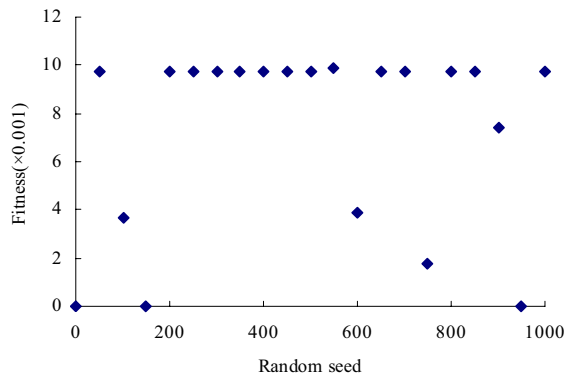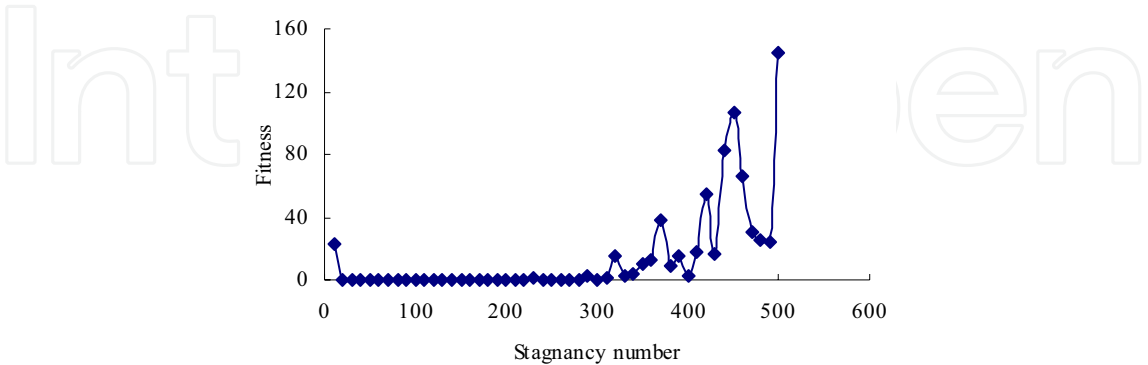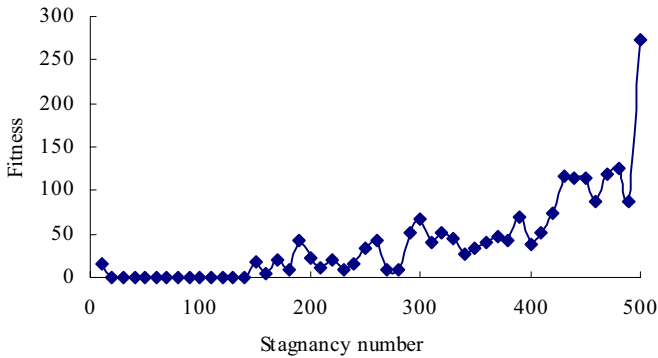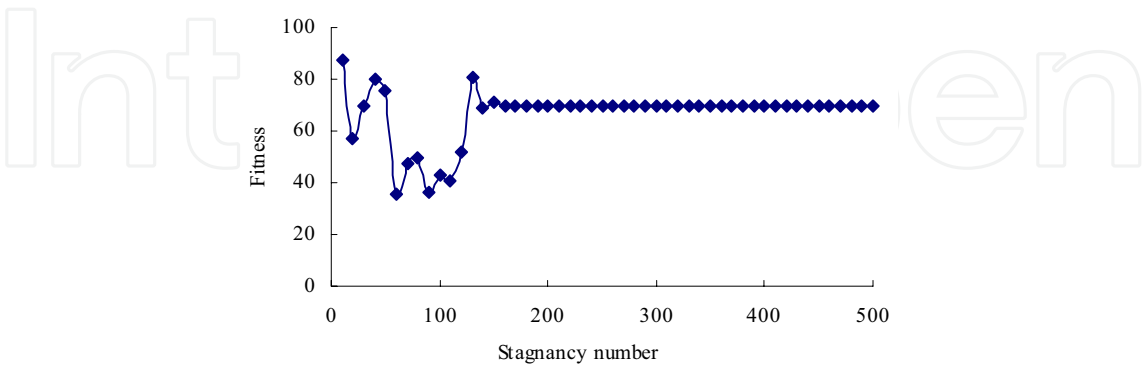Figure 4. Effect of different random seed on precision of function *Griewank*

Figure 5. Effect of different random seed on precision of function *Schaffer'f$_6$*

The effects of random seeds on performance of algorithm for five functions are shown in Fig. 1 to Fig. 5. It is obviously that random seed greatly affects the convergence velocity and precision of the CSV-PSO. If random seed is appropriate, convergence velocity of CSV-PSO is quite fast; otherwise, convergence is slower and divergence is also probable. However, this effect is random and doesn't comply with any distinctive laws.

3.4.2 Stagnancy Number N_s

In process of optimization, the best particle may not move toward any direction during a short-term flying before goal value is obtained. This is named stagnancy phenomenon. To obtained the global goal value quickly, it is necessary to initialize part of the particles once more to break this temporary stagnation. But no final conclusion about the how many the stagnancy number is has yet been reached. How to determine stagnancy number N_s will be discussed in this section by taking the functions in table 1 as examples.

	Sphere	Rosenbrock	Rastrigin	Griewank	Schaffer's f_6
Optimal value	13982.13	123073.22	264.40	126.83	9.71E-3

Table 4. Optimal value of 5 functions when stagnancy number is 1

Figure 6. Effect of different stagnancy number on precision of function *Sphere*

Figure 7. Effect of different stagnancy number on precision of function *Rosenbrock*

Figure 8. Effect of different stagnancy number on precision of function *Rastrigrin*
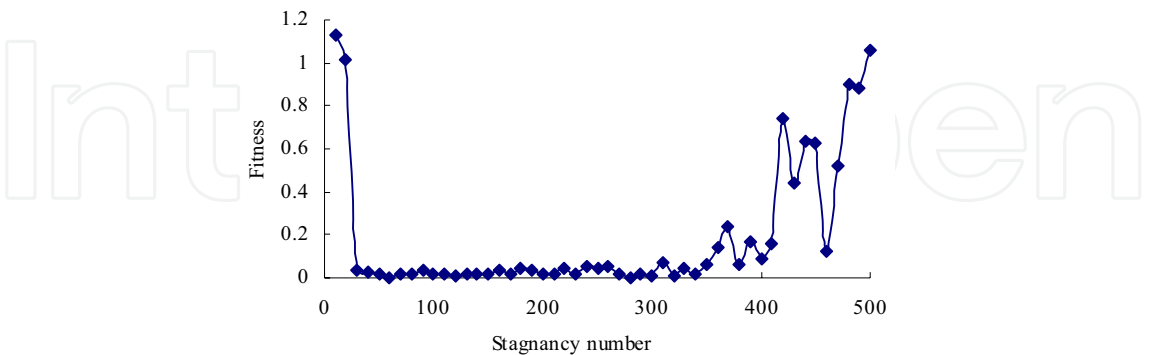
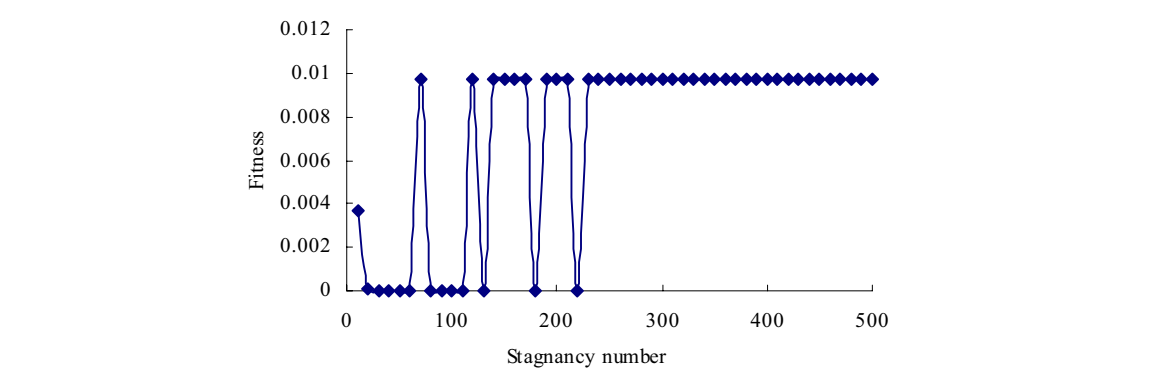Figure 9. Effect of different stagnancy number on precision of function *Griewank*

Figure 10. Effect of different stagnancy number on precision of function *Schaffer'f₆*

Most of the parameters in this section are set to be the same value as section 3.4.1 except for random seed and stagnancy number. Random seed is set to 100 and stagnancy number is set to be from 1 to 501 by an increment 10 for each solution. How the stagnancy number affects the convergence precision is indicated in Fig. 6 to Fig. 10. Because when the stagnancy number is 1, the optimal value is still very large at reaching end conditions, so these values are listed in table 4 separately.

Much numerical simulation has shown that there is stagnancy during the flight of particles. It is concluded that it is very important what time initializing part of particles is. If part of particles are initialized again when stagnancy just now happens (e.g. stagnancy number is 1.) during flight of particles, performance of CSV-PSO is least desirable and the algorithm is hard to converge. However, if the initializing is too late (e.g. stagnancy number is 500), the algorithm is also not stable and easily divergent, which are seen from table 4 and Fig. 6 to Fig. 10. The whole range can be divided into three intervals [1, 30], [30,120] and (120,501].The proposed algorithm is not easy to converge at intervals [1, 30) and (120,501] and has a trend that convergence becomes more and more difficult along with the increasing of stagnancy number at interval (120,501]. So it is suggested that initializing part of particles once again with stagnancy number between 30 and 120 will achieve better convergence.

3.4.3 Constant α_0

Constant α_0 is a parameter that determines limit of flying velocity of particles, which is shown by Eq. (6), (7) and (8). Many numerical tests show that different α_0 result in different velocity and precision of convergence in CSV-PSO. Parameters of CSV-PSO different from section 3.4.2 are stagnancy number and constant α_0 which are set to 20 and from 0 to 3.0 by an increment 0.1 for each scheme separately. And the α can be decreased without limitation by Eq. (8). The optimal values of each function vary with increasing of constant α_0 as shown in Fig. 11 to Fig. 15. As being comparatively large when constant α_0 is 0, optimal values for five functions are listed separately in table 5.

	Sphere	Rosenbrock	Rastrigrin	Griewank	Schaffer's f_6
Optimal value	51773.71	1690084.40	373.47	466.96	5.04 E-2

Table 5. Optimal value of 5 functions at α_0 =0
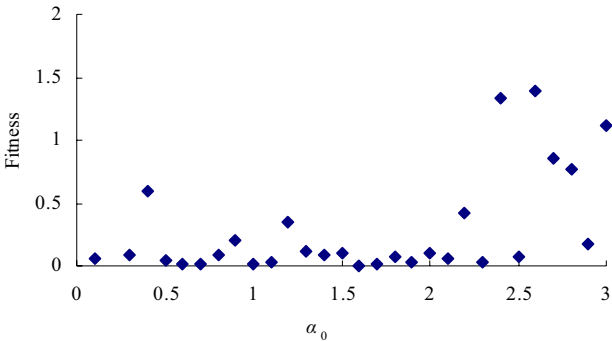
Figure 11. Effect of different constant α_0 on precision of function *Sphere*
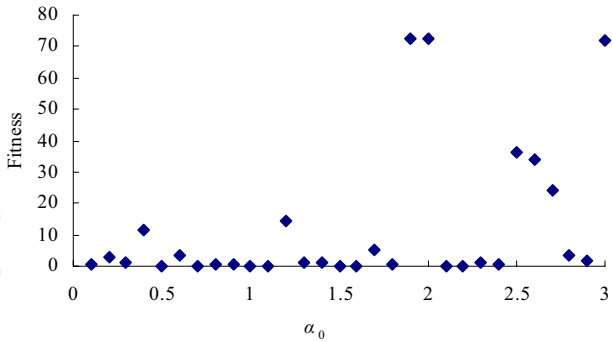
Figure 12. Effect of different constant α_0 on precision of function *Rosenbrock*

It is concluded that convergence precision of CSV-PSO for each function is very poor at meeting end condition of iteration when α_0 is 0 from table 5. If iteration continues, given goal value is also obtained hardly. This is because PSO has had no optimizing capacity when α_0 is 0, which is in accordance with the principle of the algorithm. Particles move

toward an object by mainly interaction among particles. When α_0 is 0, the upper and lower limits of particles' velocity are both zero indicated by formula (6), (7) and (8), further the velocity of flying is also zero, and locations and velocities of particles can't both be updated. So that the whole population are stagnant and the PSO finally loses optimizing capacity.
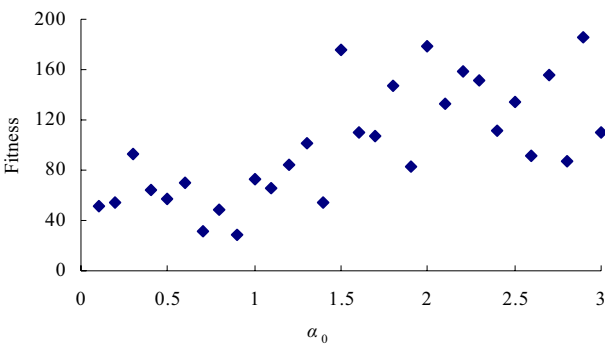

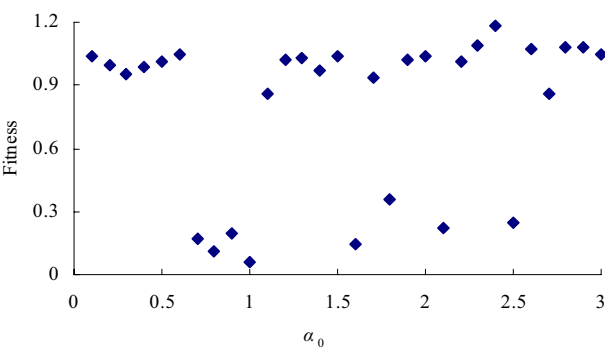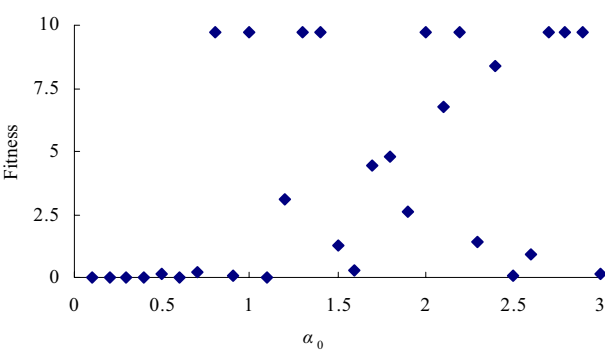Figure 13. Effect of different constant α_0 on precision of function *Rastrigrin*

Figure 14. Effect of different constant α_0 on precision of function *Griewank*

Figure 15. Effect of different constant α_0 on precision of function *Schaffer'f_6*

It is shown that the convergence capability of CSV-PSO undergoes three stages approximately along with the increasing of α_0 by Fig. 11 to Fig. 15. The first stage is at interval [0, 0.5) and convergence of the algorithm is unstable. Some functions can converge quickly to goal value while others will not in this stage. CSV-PSO has more stable convergence at interval [0.5, 1] for five testing functions. Convergent capability of the algorithm becomes much more poor and unstable when α_0 is more than 1. So interval [0.5, 1.0] is proposed.

In addition, numerical calculation indicates that if population scale is too small, algorithms may converge difficultly and the precision is bad, so enlarging the population can improve the convergence capability and enhance the precision of the algorithm; increasing iteration number can also improve the precision of the algorithm to some degree.

4. PCSV-PSO

Although the convergence speed and precision of the CSV-PSO have been are further improved, it is necessary to further improve calculation efficiency for some practical engineering application consuming a large amount of calculation time (such as rheology parameters back analysis, seepage simulation, etc.). Therefore, a parallel CSV-PSO algorithm based on MPI(Message Passing Interface, named PCSV-PSO), is proposed in the paper. As the calculations for parameter recgnition are mainly consumed in evaluation of particles' fitness, global parallel strategies (master-slave mode) is adopted in CSV-PSO algorithm in the paper. MPI is one of the most popular parallel techniques based on message passing mechanism (Du, 2001). It offers a criterion of message passing programming, which has nothing with languages and platforms, and can be widely accepted. In addition, it codes are practical, transplantable, high-efficiency and flexible.

Operation procedure can be simply introduced as following:

Firstly, the host computer allocates assignments for each process according to formula (12):

$$N^{'} = \frac{N}{m} \tag{12}$$

Where N is the total number of assignments produced by CSV-PSO (namely N groups of schemes for problems to be solved), m is the number of personal computers(PC) participating in parallel calculation, $N^{'}$ is the number of assignments of each process.

Secondly, each process executes its assignments separately, and the calculation result will be evaluated by formula (13) (That is evaluation of solutions of problem.).

$$F(x) = \sum_{i=1}^{n} \left[f_i(X) - u_i \right]^2 \tag{13}$$

In which, $f_i(X)$ and u_t are calculation value and observed object value respectively; n is the total number of observed object value.

Then, the calculating result of each process is taken back, and position, velocity, velocity limit and searching space of particles and inertia weight are updated according to Eq. (1),(2) and (5) to (10) on master PC.

Finally, determine whether the result can meet the requirement of calculation. If so, terminate the parallel calculation; otherwise, allocate new assignments to slave computers, and begin new iteration.Repeat the above processes until the requried optimization solution is obtained.

By using the above proposed method, fitness calculation of particles (one group of solved schemes for problems) is independent in each PC, wherears evaluation of all particles and all operation(such as updating of position, velocity, velocity limit and search space of particles and inertia weight, etc) are executed only by master PC. The host PC communicates with slave PCs only when allocating assignments and taking back result. Thus reduces the communication overhead prominently. Hence, the efficiency of parallel calculation is high.

5. Application of PCSV-PSO in Geotechnical Engineering

Rock is a typical complex anisotropic natural geological material including all kind of fissures, joints and defects, so mechanical characteristic and physical property are obviously different for different rocks, even if for the same rock. Hard brittle rock buried deeply under high ground stress has a greater chance of rockburst when surrounding condition of rock is changed by excavation, artificial blasting or other factors. While soft and weak rock shows another mechanics property, which deformation increases under constant stress condition or stress decreases under constant deformation condition gradually with time in long-term run of rock engineering, named time dependant characteristic. For accurate describing physical and mechanical property and learning deformation laws *in situ* of studied rock, back analysis based on measured information *in situ* is used widely in geotechnical field and many achievements have been obtained (Wang & Yang, 1987; Gavrus et al., 1996; Deng et al., 2001; Liu et al., 2005). Measured displacement regarded as the goal, back analysis method for rheological parameters of rockmass based on FLAC3D codes using PCSV-PSO is introduced firstly. Then this method is used for inversing rheological parameters of argillite at the No. 72 testing tunnel of left bank slope, Longtan Hydropower station, China.

5.1 Back Analysis of Rheologcial Parameters of Rockmass Based on PCSV-PSO

It is essential for inversing analysis method that searching a set of parameters makes calculated response accord with actual response in the whole space using an optimal technique. So for time dependant engineering problem, goal function used as back analysis can be written as following:

$$F(x) = \sum_{i=1}^{n} \sum_{t=0}^{T} \left[f_{it}(X) - u_{it} \right]^2 \tag{14}$$

Where X is a set of parameters required for inversing analysis; $f_{it}(X)$ and u_{it} are calculated displacement and measured displacement of the No. i monitoring site at t time respectively; n is total number of monitoring sites and T is total time for monitoring.

The back analysis method which is based on FLAC3D solver with PCSV-PSO can be described as following (also seen from Fig. 16):

Step 1: Initializing parameters of PCSV-PSO and ranges of parameters requiring to be analyzed inversely;

Step 2: Initializing position and velocity of particles, population size N, namely N sets of parameters requiring to be analyzed inversely;

Step 3: Host PC allocates missions to m-1 slave PC and itself. N/m missions are allocated to each PC;

Step 4: Invoking FLAC3D solver and calculating displacement of key points;

Step 5: Calculating fitness of particles by formula (14), and return the result to host PC;

Step 6: If the fitness is less than given value or iteration number is larger than maximum iteration number given, a set of optimal parameters is selected out by rheology mechanics characteristic of rock and some engineering experiences and back analysis is finished; otherwise, go to step 7;

Step 7: Updating limit of velocity, searching space and position and velocity of each particle inertia weight and so on, then go to step 3.
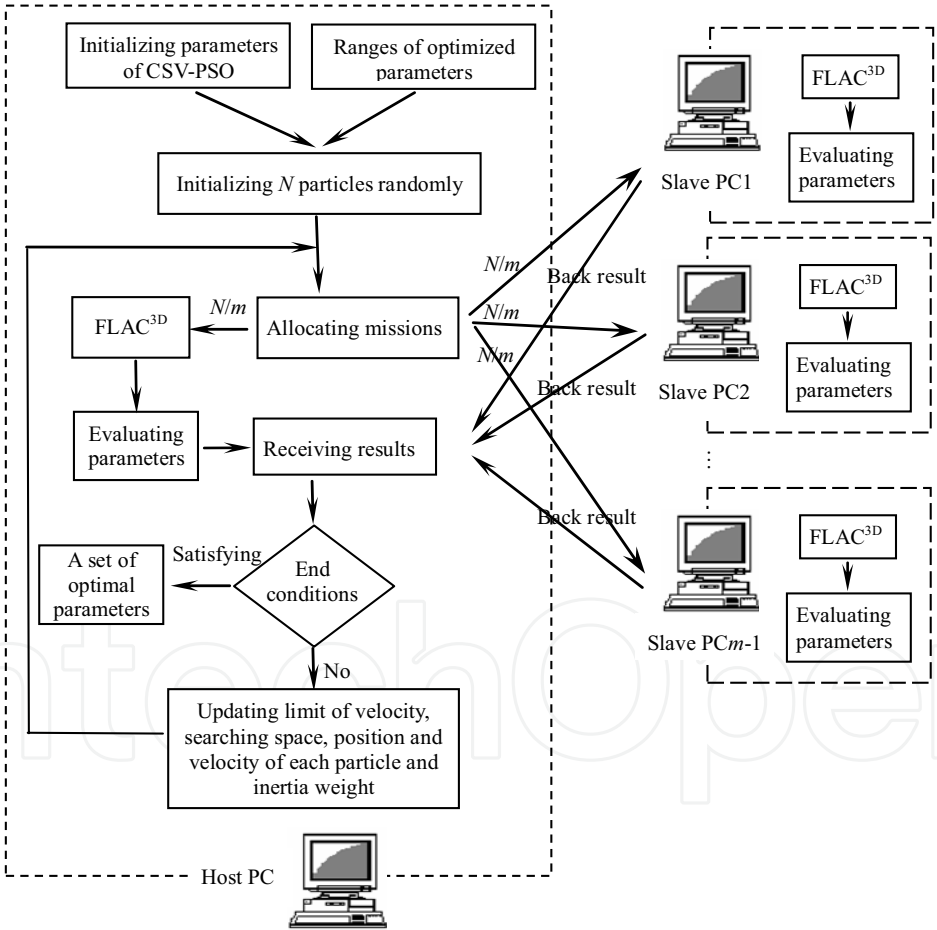
Figure 16. Flow chart of back analysis of parameters based on FLAC3D using PCSV-PSO

5.2 An application in Geotechnical Engineering

5.2.1 Introduction of Longtan Hydropower Project
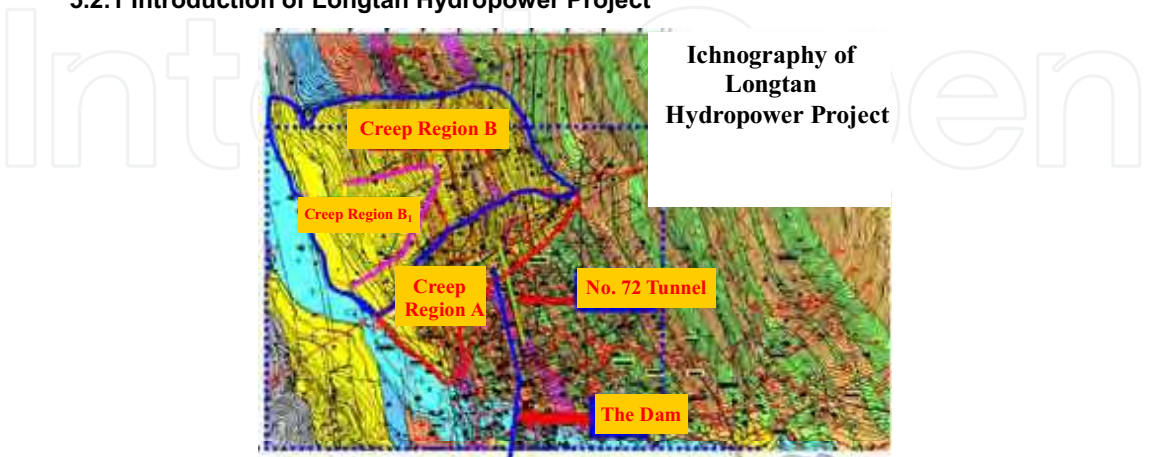
Figure 17. Distributing of creep regions of left slope at Longtan Hydropower Project

Longtan Hydropower Project, which is an important one in the implementation of national Great Western Development and the Power Transmission Project from West to East, is located in Tian'e county of Guangxi Autonomous Region, upstream of Hongshui River. It is the second largest hydropower project under construction in China, next to Three Gorges Project. The height of mountains is about 600m at both sides of the dam site. Slope on the left bank is 420m high and the slope angle is between 28 to 37 degrees, with a thickness of residual diluvial layer between 0.5 and 2m and locally from 8 to 25m. More than 500 faults are exposed in the Dam Area and about 50 ones of them are bigger. There are two big creep regions with sandstone and shale of Middle-lower Triassic Formation near dam site in the left of whole reservoir region, named creep regions A and B, which is shown as Fig. 17.
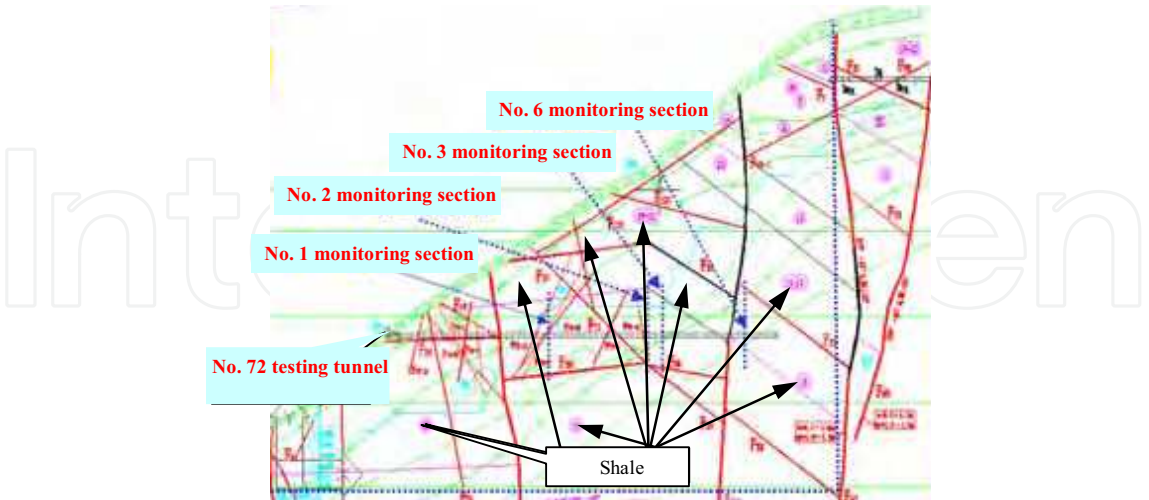
Figure 18. Engineering geological profile at location of No.72 testing tunnel
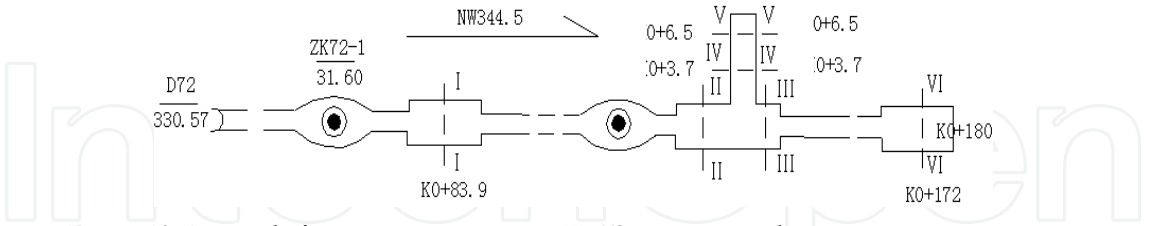
Figure 19. Disposal of monitoring sections at No.72 testing tunnel
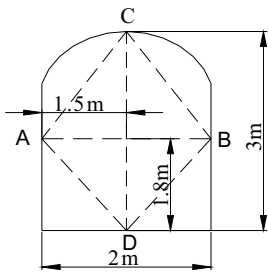
Figure 20. Disposal of survey lines at each monitoring section

As the geological conditions are quite complicated in this region, in order to know the geological conditions, rockmass physical and mechanical property, deformation characteristics and strike variation, the No.72 exploratory testing tunnel was excavated in one of the two creep regions on the left bank. Its location is shown in Fig. 17 and the main faults and strata which it passes through are shown in Fig. 18.

The No.72 test tunnel locates in the core of the left bank high slope, which is surrounded by shale and all of its 6 monitoring sections are also surrounded by shale mainly. The main tunnel is 180m long, and the branch tunnel is 136m far from the opening. The monitoring sections Ⅰ, Ⅱ, Ⅲ and Ⅵ, whose size is 2m width and 3m height, are located at 83.9, 132.4, 139.4 and 172m far from the opening of main tunnel and the monitoring sectionsⅣ and Ⅴ, having 2 m×2m sizes, are 3.7 and 6.5m far away from the opening of branch tunnel as shown as Fig. 19. The shape of all profiles is city gate. The measuring method is that the six convergent survey lines are fixed on four points of each profile. The survey lines are disposed as Fig. 20.

5.2.2 Numerical Calculation Model

To eliminate the boundary effect as much as possible, calculation ranges in which width is 100m at X direction, length is 280m at Y direction and height is from 240m yellow sea height to slope surface at Z direction is determined. The calculation region is shown in Fig. 21 in horizontal plane. 3D Meshes are generated in terms of the calculation region determined above, which contain 37343 elements and 8601 nodes of meshes. Local mesh refinement technique is used near six monitoring sections. Solid elements are used to simulate faults having some thickness. The model of calculation mesh of the whole ranges is shown in Fig. 22. Distribution of faults and test tunnels in calculation range is displayed in Fig. 23.

Initial stress fields adopt 3D initial stress fields regressed by Hu et al. (Hu et al., 2005). Bottom surface, planes vertical to X-axis and Y-axis are all constrained at normal direction and natural slope surface is free. According to deformation monitoring data *in situ*, testing tunnels go through instant elastic, attenuation and relatively stable deformation three

stages. Therefore, the combined model of Kelvin-Voigt model for viscoelastic property of rock and Mohr-Coulomb model which is used to express plastic characteristic of material is adopted to describe viscoelastic plastic property of shale as Fig. 24.
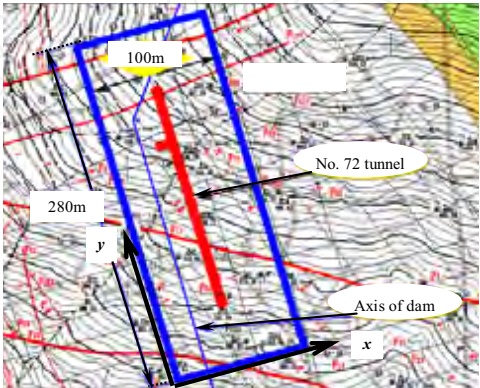

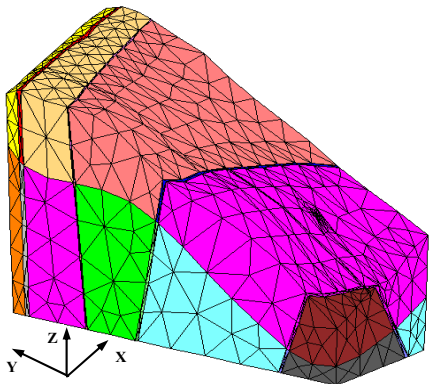Figure 21. Calculation region for numerical model of the No.72 testing tunnel

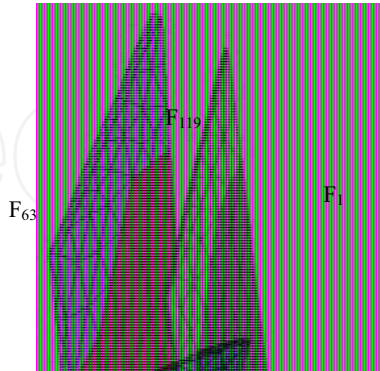

Figure 22. Three-dimension mesh model for calculation

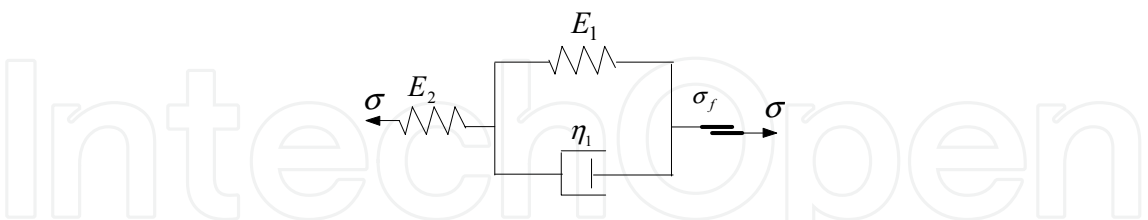Figure 23. Distribution of faultages and testing tunnels

Figure 24. Combined model for describing viscoelastic-plastic characteristic

According to excavation schemes, monitoring data and the feasibility of numerical simulation, 180m-long NO.72 testing tunnel is excavated by 13 stages and each stage is finished once. As displacement monitoring is later than excavation and instant deformation of surrounding rock can't be reflected in displacement monitoring, proper measure must be taken to make process of numerical simulation agree with that of monitoring *in situ*.

FLAC3D of the *ITASCA* company is used as a solver when numerical simulation starts. For each excavation, elastic and plastic analysis is carried out at first followed by rheological calculation. Strong weathered, weak weathered, slightly weathered shale and fresh sandstone interbedded with fresh shale four kinds material are considered for elastic and plastic calculation. Fully weathered and strong weathered shale are regarded as the same material and weak weathered and fresh shale are regarded with the same property in viscoelastic plastic numerical simulation. Several large faults F_1、F_4、F_{63} and F_{119} crossed by the No.72 testing tunnel are taken into concern in elasticplastic and viscoelastic plastic simulations.

5.2.3 The goal of back analysis

As excavation and all kind of artificial factors, monitoring data are not full and have big variations in profiles II and IV. In addition, the distance of profiles II and III and location of profiles IV and V are very close and profiles IV and V are in the branch tunnel, therefore, only monitoring data of profiles I, III, V and VI are selected as the goal of back analysis, where only suvey lines AD,BD and CD of the first profile, suvey lines AC,CD and BD of the third profile, suvey lines AB,CD,AC and BC of the fifth profile and suvey lines AD and CD of the sixth profile are used as effective survey lines. The goal function of back analysis is described by formula (14).

5.2.4 Identification of Parameters of Constitutive Model

For Mohr-Coulomb model, mechanical property parameters of strong weathered, weak weathered, slightly weathered shale, fresh sandstone interbedded with fresh shale and the four faults are determined as listed in table 6 based on geological conditions and mechanical testing, in which elastic modulus are the same as elastic modulus of each rock in series branch of viscoelastic model and is gained by latter inversing analysis.

For Kelvin-Voigt model, its parameters are recognized using displacement back analysis method with PCSV-PSO as mentioned in section 5.1. Total eight PCs which are equipped with 2.8GHz CPU, 512MB memory, 10MBps/100MBps net card and 80GB hard disk participate in this parallel calculation of inversing analysis. Other equipments include a HUB with 16 interfaces, a 17 inch terminal, a manual control switch and some net wires, etc.

Sorts of rockmass	Unit	Tensile	Shear strength	Poisson's

	weight (kN·m⁻³)	strength (Mpa)	Friction angle(°)	C(Mpa)	ratio
Strong weathered shale	25.5	0.08	36.9	0.49	0.34
weak weathered shale	26.5	0.8	50.2	1.18	0.28
slightly weathered shale	26.8	0.8	47.7	1.48	0.26
fresh sandstone with fresh shale	26.9	1.3	52.4	1.96	0.25
Faults F_1、F_4、F_{63} and F_{119}	21	0	18	0.04	0.34

Table 6. Property of several rockmass for Mohr-Coulomb model

Before the parameters are identified using swarm intelligence method, they must have ranges themselves. The ranges of parameters of Kelvin-Voigt model are determined by engineering experience, geology investigation, rock testing in laboratory and in field and a small amount of numerical calculation, as shown in table 7.

Fully and strong weathered shale			Weak weathered and new shale		
E_1(GPa)	η_1 (GPa.d)	E_2 (GPa)	E_1(GPa)	η_1 (GPa.d)	E_2 (GPa)
20-40	5-20	1-15	80-110	5-20	5-20

Table 7. Ranges of parameters of Kelvin-Voigt model for the two rockmass

The parameters of PCSV-PSO are set as follows: the maximum number of iteration is 20, the population size is 16, learning factors c_1 and c_2 are both 2.0, initial inertia weight is 1.0, constants α_0 and β_0 are set to be 0.9 and 0.8 respectively, random seed is set to be 100 and the maximum stagnancy number is 10.

Fully and strong weathered shale			Weak weathered and new shale		
E_1(GPa)	η_1 (GPa.d)	E_2 (GPa)	E_1(GPa)	η_1 (GPa.d)	E_2 (GPa)
31.90	9.02	5.82	92.52	78.41	12.98

Table 8. Recognized parameters of Kelvin-Voigt model for the two rockmass
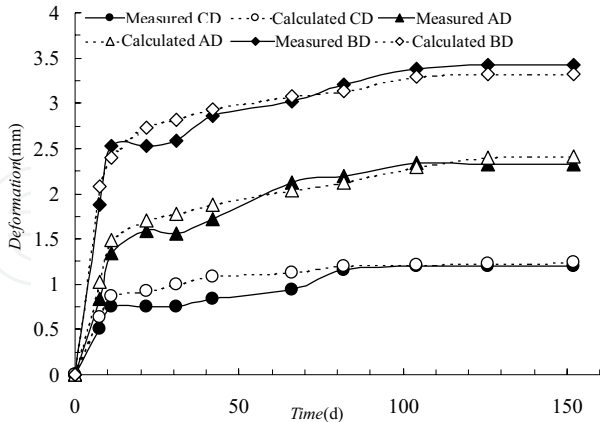

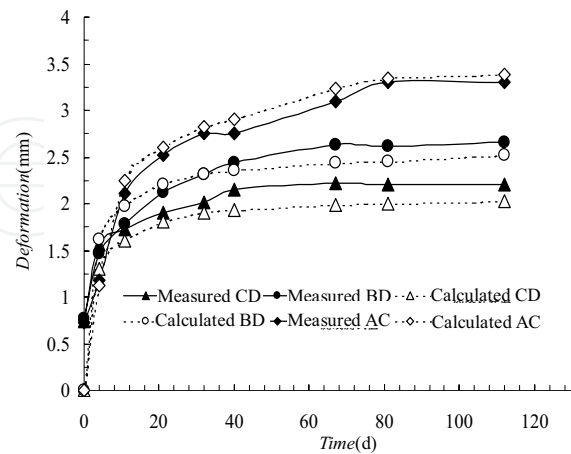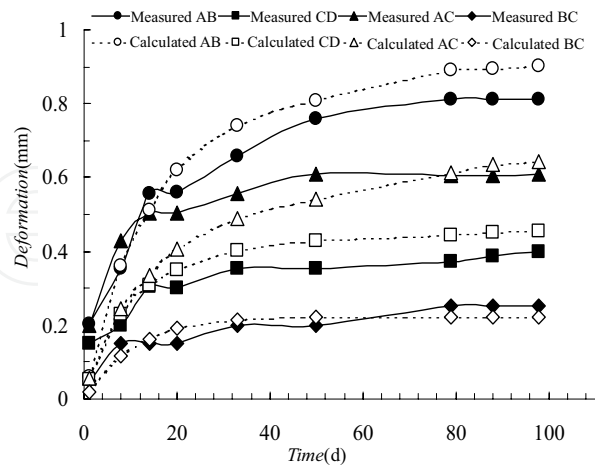Figure 25. Comparison calculated deformation with monitored it at profile I

Figure 26. Comparison calculated deformation with monitored it at profile Ⅲ

As numerical simulation of rock rheology is a time-consuming job, although maximum number of iteration and the population size are set to smaller values, it still consumes almost two days until the final parameters of the two rocks are obtained using the proposed method in section 5.1. If finishing a scheme needs 50 minutes averagely, it will consume about 10 days that parameters are identified in single PC. So efficiency is improved highly using the PCSV-PSO algorithm. When iteration is executed 20 times, the final identified parameters are obtained in table 8 and the residual sum of squares of the calculated deformation and actual deformation is 9.36×10^{-5} m^2. The calculated deformation is compared with actual deformation, as shown in the Fig. 25 to Fig. 28. It is concluded that the calculation result of all survey lines of the four profiles is acceptable for practical engineering, the simulating trend of deformation with the above identified parameters accords with that recorded in the field from Fig. 25 to Fig. 28 and the proposed algorithm is a faster and more efficiency back analysis method for identifying parameters.

Figure 27. Comparison calculated deformation with monitored it at profile Ⅴ
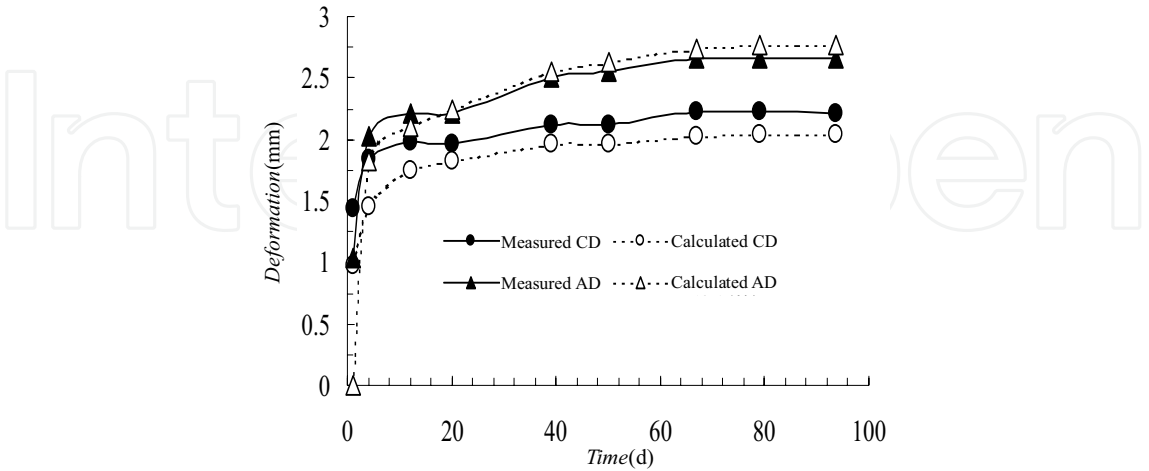
Figure 28. Comparison calculated deformation with monitored it at profile VI

6. Conclusion

Two modified versions of PSO are introduced: one is CSV-PSO algorithm in which random numbers are generated by the mixed congruential method, and another is PCSV-PSO algorithm for recognizing rheological parameters of rockmass. A great deal of numerical simulations show that the CSV-PSO algorithm has better convergence performance and more accurate convergence precision, its run is more stable and it can provide certainty solution in different runtime. Sensitivity analysis of the CSV-PSO algorithm indicates that random seed, stagnancy number and constant α_0 determining flying velocity of particles have a great effect on performance of the algorithm. Proper random seed can accelerate convergence of the algorithm; while bad random seed can not only slow convergence velocity but also possibly result in divergence. However, no obvious law can be followed. If the stagnancy number is too small or too large, the algorithm is hard to converge and unstable. The interval in which the algorithm converges more easily is [30,120]. If the constant α_0 is smaller in interval [0, 0.5], the optimizing capability of the algorithm is poorer and if the constant α_0 is zero, the algorithm loses optimizing capability. However, if constant α_0 is too large, the velocity of particles will be large so that the algorithm can't also unstably converge. That interval [0.5, 1.0] is suggested is proper for convergence of the algorithm. Based on monitoring information in situ, identifying mechanical parameters of rockmass using back analysis technique is a time-consuming task. Rheological parameters of the two rocks at the No.72 testing tunnel of left bank slope, Longtan Hydropower Station, China, as an example, are identified using the PCSV-PSO algorithm. The results indicate PCSV-PSO algorithm is a new feasible and high efficient analytical tool for solving geotechnical engineering problem.

7. Acknowledgement

8. References

Chen B R, Feng X T (2005). Particle swarm optimization with contracted ranges of both search space and velocity. *Journal of Northeastern University (Natural Science)*, Vol.26, No.5,pp.488-491.

Clerc M (1999). The swarm and the queen: towards a deterministic and adaptive particle swarm optimization, *Proc. 1999 Congress Evolutionary Computation*,pp. 1951-1957, Piscataway,1999, NJ: IEEE Press.

Clerc M, Kennedy J (2002). The particle swarm: explosion, stability, and convergence in a multidimensional complex space. *IEEE Transations on Evolutionary Computation*,Vol.6, No.1, pp. 58-73.

Deng J, Lee C F, Ge X (2001). Disturbed Zones and Displacement Back Analysis for Rock Slopes. *Chinese Journal of Rock Mechanics and Engineering*, Vol.20, No.2, pp. 171-174.

Dong Y, Tang J, Xu B, et al. (2003). Application of Particle Swarm Optimization to Nonlinear Constrained Programming. *Journal of Northeastern University (Natural Science)*, Vol.24, No.12, pp. 1141-1144.

Du Z (2001). MPI Parallel Programming : High Performance Computation and Parallel Program Technique. Tsinghua University Press, Beijing.

Eberhart R C, Kennedy J. P.(1995). A New Optimizer Using Particle Swarm Theory.In: *Proc. of the Sixth International Symposium on Micro Machine and Human Science*,pp.39-43, Nagoya,Japan.

Eberhart R C, Shi Y (2000). Comparing inertia weights and constriction factors in particle swarm optimization. *Proc. 2000 Congress Evolutionary Computation,* pp.84-88, Piscataway, 2000,NJ: IEEE Press.

Gavrus A., Massoni E. and Chenot J. L. (1996). An inverse analysis using a finite element model for identification of rheological parameters. *Journal of Materials Processing Technology*, Vol.60, No.1-4,pp. 447-454.

Hu B, Feng X T, et al. (2005). Regression Analysis of Initial Geostress Field for Left Bank High Slope Region At Longtan Hydropower Station. *Chinese Journal of Rock Mechanics and Engineering*, Vol.24, No.22, pp.4055-4064.

Ke J, Qian J X, Qiao Y Z (2003). A Modified Particle Swarm Optimization Algorithm. *Journal of Circuits and Systems*, Vol.8, No.5, pp. 87-91.

Kennedy J, Eberhart R C (1995). Particle Swarm Optimization. *Proc. IEEE Int. Conf. Neural Networks*, pp.1942-1948, Piscataway, 1995, NJ: IEEE Press.

Liu Q J, Yang L D, Cao W G (2005). Statistical Damage Constitutive Model For Rock and Back Analysis of Its Parameters. *Chinese Journal of Rock Mechanics and Engineering*, Vol.24, No.4, pp.616-621

Lovbjerg M, Rasmussen T K, Krink T (2001). Hybrid Particle Swarm Optimizer With Breeding and Subpopulations. In: *Proc. of the third Genetic and Evolutionary Computation Conference*, pp.469-476, San Francisco.

Lü Z S, Hou Z R (2004). Particle Swarm Optimization with Adaptive Mutation. *Acta Electronica Sinica*, Vol.32, No.3, pp.416-420.

Mark S V, Feng X (2002). ARMA model selection using particle swarm optimization and AIC criteria. *15th Triennial World Congress*, pp.117-129, Barcelona, 2002, Spain: IFAC.

Wang S, Yang Z (1987). The back analysis method from displacement for viscoelastic rock mass. In: *Proc 2nd Int Symp on FMGM'87*,pp.1059-1068.

Su G, Feng X (2005). Parameter Identification Of Constitutive Model For Hard Rock Under High In-Situ Stress Condition Using Particle Swarm Optimization Algorithm. *Chinese Journal of Rock Mechanics and Engineering*,Vol.24,No.17, pp.3029-3034.

Shi Y, Eberhart R C(1998). A Modified Particle Swarm Optimizer. In: *IEEE World Congress on Computational Intelligence*, pp.69-73,Anchorage, Alaska.
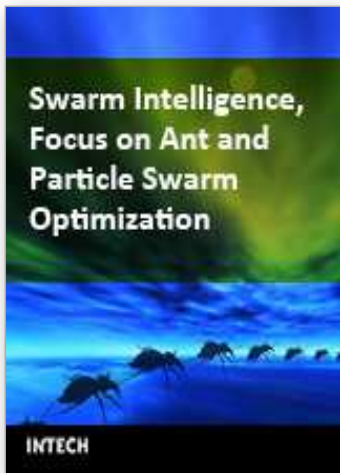
Swarm Intelligence, Focus on Ant and Particle Swarm Optimization

Edited by FelixT.S.Chan and Manoj KumarTiwari

ISBN 978-3-902613-09-7

Hard cover, 532 pages

Publisher I-Tech Education and Publishing

Published online 01, December, 2007

Published in print edition December, 2007

In the era globalisation the emerging technologies are governing engineering industries to a multifaceted state. The escalating complexity has demanded researchers to find the possible ways of easing the solution of the problems. This has motivated the researchers to grasp ideas from the nature and implant it in the engineering sciences. This way of thinking led to emergence of many biologically inspired algorithms that have proven to be efficient in handling the computationally complex problems with competence such as Genetic Algorithm (GA), Ant Colony Optimization (ACO), Particle Swarm Optimization (PSO), etc. Motivated by the capability of the biologically inspired algorithms the present book on "Swarm Intelligence: Focus on Ant and Particle Swarm Optimization" aims to present recent developments and applications concerning optimization with swarm intelligence techniques. The papers selected for this book comprise a cross-section of topics that reflect a variety of perspectives and disciplinary backgrounds. In addition to the introduction of new concepts of swarm intelligence, this book also presented some selected representative case studies covering power plant maintenance scheduling; geotechnical engineering; design and machining tolerances; layout problems; manufacturing process plan; job-shop scheduling; structural design; environmental dispatching problems; wireless communication; water distribution systems; multi-plant supply chain; fault diagnosis of airplane engines; and process scheduling. I believe these 27 chapters presented in this book adequately reflect these topics.

INTECH
open science | open minds